A PROPOSED FABRICATION METHOD OF NOVEL PCL-GEL-HAp NANOCOMPOSITE SCAFFOLDS FOR BONE TISSUE ENGINEERING APPLICATIONS

A. Hamlekhan*, M. Mozafari*, N. Nezafati, M. Azami, H. Hadipour

Biomaterials Group, Faculty of Biomedical Engineering (Center of Excellence), Amirkabir University of Technology, P. O. Box: 15875-4413, Tehran, Iran

*Authors to whom correspondence should be addressed
E-mail: mmozafari@aut.ac.ir

Received 3 April 2010; accepted 27 July 2010

ABSTRACT

In this study, poly(ε-caprolactone) (PCL), gelatin (GEL) and nanocrystalline hydroxyapatite (HAp) was applied to fabricate novel PCL-GEL-HAp nanaocomposite scaffolds through a new fabrication method. With the aim of finding the best fabrication method, after testing different methods and solvents, the best method and solvents were found, and the nanocomposites were prepared through layer solvent casting combined with freeze-drying. Acetone and distillated water were used as the PCL and GEL solvents, respectively. The mechanical test showed that the increasing of the PCL weight through the scaffolds caused the improvement of the final nanocomposite mechanical behavior due to the increasing of the ultimate stress, stiffness and elastic modulus (8 MPa for 0% wt PCL to 23.5 MPa for 50% wt PCL). The biomineralization investigation of the scaffolds revealed the formation of bone-like apatite layers after immersion in simulated body fluid (SBF). In addition, the *in vitro* cytotoxity of the scaffolds using L929 mouse fibroblast cell line (ATCC) indicated no sign of toxicity. These results indicated that the fabricated scaffold possesses the prerequisites for bone tissue engineering applications.

Keywords: Nanocomposite; Fabrication; Poly(ε-caprolactone); Gelatin; Hydroxyapatite; In vitro study

1. INTRODUCTION

Despite the wide use of porous biomaterials as nanocomposite scaffolds, the design and optimization of scaffolds for successful integration remain an inexact science. Criteria which must be considered in the design of biomaterials include the provision of adequate mechanical properties, the inclusion of adequately large pore volumes to accommodate and deliver a cell mass sufficient for tissue engineering applications, adequate biocompatibility and biodegradability. Various nanocomposite scaffolds can be fabricated using bioactive fillers and also blends of synthetic and natural polymers by choice of suitable solvents and fabrication methods. Nanocomposite scaffolds which blend synthetic and natural polymers can exploit the advantages of both polymer types [1]. In addition, applying bioactive materials throughout the nanocomposite matrixes especially HAp can extremely improve the bone regeneration ability of these materials. Nowadays, the application potential of scaffolds made from blends of synthetic and natural polymers for tissue regeneration have been investigated by many researchers [3–4].

GEL is a natural biopolymer derived from collagens by controlled hydrolysis [5]. Because of its many merits, such as its biological origin, biodegradability, biocompatibility, and commercial availability at relatively low cost, GEL has been widely used in biomedical applications. In pharmaceutical and medical fields, GEL has long been used as sealants for vascular prostheses [6,7], carriers for drug delivery [8], dressings for wound healing [9], and so forth. Anyway, using the approach of mixing GEL with synthetic polymers has frequently been adopted by other researchers. This is a feasible approach that may not only reduce the potential problem of cytotoxin, as a result of using a chemical cross-linking reagent, but also provide a compromise solution for overcoming the shortcomings of synthetic and natural polymers, that is, producing a new biomaterial with good biocompatibility and improved mechanical and physico-chemical properties.

Among synthetic polymers, PCL has been considered as an appropriate choice for mixing with GEL due to the fact that PCL is a semicrystalline linear

resorbable aliphatic polyester, and subjected to hydrolytic degradation because of the susceptibility of its aliphatic ester linkage to hydrolysis [10,11]. On the other hand, PCL is regarded as a soft and hard biocompatible material for tissue engineering applications because of resorbable suture, drug delivery system and also bone-graft substitutes [12]. Although applications of PCL might be limited because its degradation and resorption kinetics are considerably slower than other aliphatic polyesters, due to its hydrophobic character and high crystallinity, PCL is currently under study for use as a potential material for bone regeneration.

On the other point of view, Biomaterials research field focus on the synthesis of bioactive ceramics based on calcium phosphates (CaP) particularly in the composition of HAp [$Ca_{10}(PO_4)_6(OH)_2$] for three decades to applications in orthopedics and dentistry [13,14]. However, it is difficult to handle and keep in defect sites because of its brittleness and low plasticity.

As mentioned above, each of the materials has been widely used in the tissue engineering scaffolds but they have their problems, so for improving these weaknesses, many works have been accomplished. For example, Causa *et al* [15] used PCL-based composites with addition of HAp particles at different volume/weight ratio. It showed both good mechanical performance and appreciable biocompatibility. In another work by Chang *et al* [16], the GEL-HAp nanocomposites were fabricated as foams. The mechanical properties of the foams and in the same research by Lia *et al* [17] the biological and mechanical properties of GEL-apatite nanofibres were examined and the result was better than using the GEL lonely, and the scaffolds also showed excellent biocompatibility and mechanical stability.

In this research, the HAp powder was synthesized by chemical precipitation through aqueous solutions of the reactants as filler. Then, to mimic the mineral and organic component of natural bone, the PCL-GEL-HAp nanocomposites were fabricated via a novel method. Then, the nanocomposite scaffolds characterized to investigate the possibility of using as bone tissue engineering scaffolds.

2. MATERIALS AND METHODS

2.1 Materials

Calcium nitrate tetra-hydrate [$Ca(NO_3)_2$.$4H_2O$, 98%], diammonium hydrogen phosphate [$(NH_4)_2HPO_4$, 99%] and sodium hydroxide [NaOH, 99%] were purchased from Merck Inc. to synthesize the HAp powder by precipitation technique. PCL used in this study were obtained from Solvay with an average molecular weight of 50,000 (CAPA-6500). Also, GEL for microbiology (Merck No. 104070) was used. The GEL foams were cross-linked by immersing into Glutardialdehyde (GA) (Merck No. 820603). Also, Distilled water, Acetone extra pure, Dimethyl sulfoxide (DMSO), Tetrahydrofuran (THF), N, N-Dimethylformamide (DMF) and Acetic acid 100% (glacial) were purchased from Merck Inc. as polymer solvents.

2.2. Synthesis of nanocrystalline hydroxyapatite (HAp) powder

The HAp powder was prepared by chemical precipitation through aqueous solutions of the reactants. A total of 0.09 M diammonium hydrogen phosphate solution and 0.15 M calcium nitrate tetrahydrate solution were prepared and the pH of the both solutions was brought to 10 by adding a small amount of sodium hydroxide solution. The phosphate solution was added drop-wise into calcium nitrate solution, resulting in the precipitation of HAp. After ripening for a specified period of time (24 h) at room temperature, the precipitates were recovered by centrifuge and then washed with de-ionized water. Five cycles of washing and centrifuging were repeated to ensure complete removal of the by-product. The calcination of the synthesized powders was carried out at 800 °C for 1 h in air using a heating rate at 3.0 °C/min in an electrical tube furnace from room temperature to 800 °C after drying the sample in freezer-drier for 10 h.

2.3. Nanocomposite scaffolds fabrication methods

Due to the hydrophobic structure of GEL molecules and the hydrophilic structure of PCL molecules, applying of these two polymers as a nanocomposite had been too challenging. Thus, several preliminary methods were investigated to determine the best fabrication method of by using different solvents. These methods are mentioned in detail in Table 1. In this effort, the eighteenth method has brought into focus.

After finding the best fabrication method, the GEL of 10% (w/v) was added into distilled water and stirred at 40°C for 1 h. HAp nanoparticles were added to the solution at 40 wt% of the GEL. The mixture was homogenized in an ultrasonic place by a stirrer at 40 °C for 1 h. The GEL-HAp solution was poured into plastic dishes and left in ambient conditions for 10 min to form the first GEL-HAp layer. Then, a

Table 1: Primary methods to find the best fabrication method of the nanocomposite scaffolds.

No.	PCL solvent	GEL solvent	Method	Result
1	DMSO	Distilled water	*Gradual addition of GEL solution to PCL solution*	PCL lumpy segregation
2	THF	Distilled water	*Gradual addition of GEL solution to PCL solution*	PCL lumpy segregation
3	Acetone	Distilled water	*Gradual addition of GEL solution to PCL solution*	PCL lumpy segregation
4	Acetic acid	Distilled water	*Gradual addition of GEL solution to PCL solution*	PCL lumpy segregation
5	DMF	Distilled water	*Gradual addition of GEL solution to PCL solution*	PCL lumpy segregation
6	DMSO	DMSO	*Gradual addition of GEL solution to PCL solution*	PCL light segregation
7	DMSO	DMSO	*Gradual addition of GEL solution to PCL solution-increasing stirring time*	PCL light segregation
8	DMSO	DMSO	*Gradual addition of GEL solution to PCL solution-increasing stirring rate*	PCL light segregation
9	DMSO	DMSO	*Gradual addition of GEL solution to PCL solution□sudden cooling*	PCL tiny segregation
10	DMSO	DMSO	*Gradual addition of GEL solution to PCL solution□decreasing PCL percentage*	PCL lumpy segregation
11	Acetic acid	Acetic acid	*Gradual addition of GEL solution to PCL solution*	PCL layer segregation and HAp dissolution
12	Acetic acid	Acetic acid	*Gradual addition of GEL solution to PCL solution□stirring during freezing*	PCL blend obtained but HAp was dissolved
13	Acetic acid	Distilled water	*Gradual addition of GEL solution to PCL solution□decreasing acidity by water*	PCL lumpy segregation in up to 80% water
14	Acetic acid	Acetic acid	*Gradual addition of GEL solution to PCL solution□decreasing acidity by ammonium*	PCL lumpy segregation
15	Acetic acid	Acetic acid	*Gradual addition of GEL solution to PCL solution□decreasing stirring time to avoid HAp dissolution*	PCL blend obtained but HAp was dissolved
16	Acetic acid	Distilled water	*Infiltration HAp slush to PCL scaffold by ultrasonic vibration*	Lack of perfect HAp infiltration
17	Acetone	DMSO	*Gradual addition of GEL solution to PCL solution*	PCL tiny segregation
18	*Acetone*	*Distilled water*	*Lamination of PCL layers between GEL layers*	*PCL-GEL blend was obtained*

solution of 10% (w/v) PCL in acetone was poured on the GEL-HAp layer and the complex was left in ambient conditions for 20 min to form the PCL layer. After evaporation of the acetone, the GEL-HAp solution was poured again to fabricate the next GEL-HAp layer. Lamination was continued to form the fourth GEL-HAp layer. After evaporation of the acetone, lots of macro porosities were observed in the surface of PCL layers which made GEL able to influence throughout the nanocomposite layers. Five samples were fabricated in which PCL amount were 0, 20, 30, 40 and 50 wt% of GEL. The samples were frozen in the freezer at -20 °C for 24 h and then moved to the freeze-drier for 72 h. The prepared samples were immersed into 1% GA aqueous solution for 24 h to crosslink the GEL-HAp layers. Finally, the cross-linked nanocomposites were carefully washed several times to remove the rest of GA and then dried in freeze-drier.

2.4. Preparation of SBF solution

The SBF solution was prepared by dissolving reagent-grade NaCl, KCl, $NaHCO_3$, $MgCl_2.6H_2O$, $CaCl_2$ and KH_2PO_4 into distilled water and buffered at pH=7.25 with TRIS (trishydroxymethyl aminomethane) and HCl 1N at 37 °C. Its composition is given in Table 2 and is compared with the human blood plasma.

Table 2: Ion concentrations of SBF and human blood plasma

Ion	*Plasma (mmol/l)*	*SBF (mmol/l)*
Na^+	142.0	142.0
K^+	5.0	5.0
Mg^{+2}	1.5	1.5
Ca^{+2}	2.5	2.5
Cl^-	103.0	147.8
HCO_3^-	27	4.2
HPO_4^{-2}	1.0	1.0
SO_4^{-2}	0.5	0.5

2.5. Characterization

The resulting HAp powder was analyzed by X-ray diffraction (XRD) with Siemens-Brucker D5000 diffractometer. This instrument works with voltage and current settings of 40 kV and 40 mA respectively and uses Cu-Kα radiation (1.540600 Å). For qualitative analysis, XRD diagrams were recorded in the interval $20 \leq 2\theta \leq 60°$ at scan speed of 2°/min being the step size 0.02° and the step time 1 s.

Transmission electron microscopy (TEM; CM200-FEG-Philips) was used for characterizing the HAp particles. For this purpose, particles were deposited onto Cu grids, which support a carbon film. The particles were deposited onto the support grids by deposition from a dilute suspension in acetone or ethanol. The particles shape and size were characterized by diffraction (amplitude) contrast and, for crystalline materials, by high resolution (phase contrast) imaging.

In order to calculate the Ca/P molar ratio of the precipitated powder, the content of Ca and P were

chemically analyzed by quantitative chemical analysis via EDTA titration technique and atomic absorption spectroscopy (AAS) with a Shimadzu UV-31005 instrument, respectively.

The functional group of nanocomposite samples were ascertained by Fourier transforms infra-red spectroscopy (FTIR). For IR analysis, in first samples were powdered and then dispersed into pellets of KBr (infrared grade) and the spectra recorded by Bomem MB 100 spectrometer in the range 400–4000 cm-1 at the scan speed of 23 scan/min with 4 cm-1 resolution.

Microstructure and morphology of porous nanocomposite (pore morphology) and measurement of pores size was evaluated using SEM analysis. For this purpose the nanocomposite samples were coated with a thin layer of Gold (Au) by sputtering (EMITECH K450X, England) and then the morphology of the samples were observed on a scanning electron microscope (SEM- Philips XL30) that operated at the acceleration voltage of 15 kV. Energy dispersive X-ray analyzer (EDX, Rontec, Germany) directly connected to SEM was used to investigate semi-quantitatively chemical compositions.

Compression strength tests were performed on the porous foams. Each sample was loaded using Zwick-Roell (MCT-25-400, Germany) at a crosshead speed of 2 mm/min with a load of 500 N cell in ambient conditions. The stress-strain curve was obtained to determine mechanical properties including elastic modulus, compression strength, maximum stress, and strain at maximum stress. The elastic modulus was obtained from the slope at the initial stages of loading (2% strain). Five specimens were tested for each nanocomposite.

2.6. Biomineralization evaluation

With the aim of investigation of bone-like apatite formation ability of the fabricated scaffolds, three scaffolds of equal weight and shape were immersed in SBF solution and incubated at 37 °C in closed Falcon tube for 3, 7 and 14 days. After the specified times, the scaffolds were removed and then carefully washed four times with de-ionized water to remove adsorbed minerals. Finally, the scaffolds were lyophilized, viewed and analyzed using SEM and EDX for mineralization.

2.7. Cytotoxicity evaluation

L929 mouse fibroblast cell line (ATCC) was used for cytotoxicity. The cells were seeded in polystyrene plates enriched with Minimal Essential Medium supplemented with 10 % fetal bovine serum,100 units/ml of penicillin and 100 µg/ml streptomycin, respectively, and then incubated at 37°C in humid atmosphere and 5% CO2. When the cells attained confluency, the sterilized scaffolds were placed in direct contact with the cells and incubated for 48 h under the same condition. Negative (Ultra High molecular weight Poly Ethylene) and positive (copper) controls were used. After 48 h, the cells were observed under optical microscopy (Nicon E200). Cellular responses were scored as 0, 1, 2 and 3 according to non-cytotoxic, mildly cytotoxic and severely cytotoxic as per ISO 10993-5.

2.8. Statistical analysis

All experiments were performed in fifth replicate. The results were given as means ± standard error (SE). Statistical analysis was performed by using One-way ANOVA and Tukey test with significance reported when $P<0.05$. Also for investigation of group normalizing, Kolmogorov-Smirnov test was used.

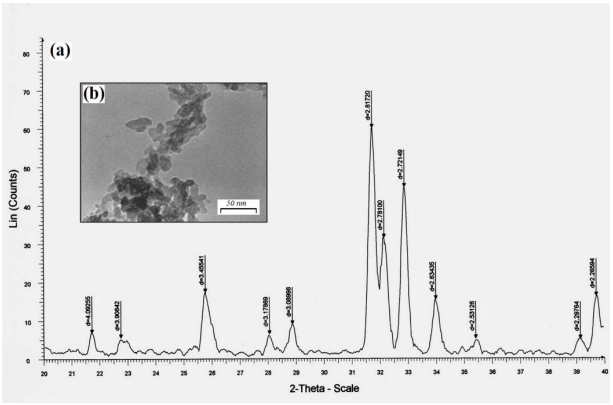

Fig. 1: (a) The XRD pattern and (b) the TEM micrograph of the synthesized nanocrystalline HAp powder

3. RESULTS AND DISCUSSIONS

3.1. HAp

The XRD data of the nanocrystalline HAp powder is presented on Fig. 1 (a). The XRD analysis was performed using an X-ray diffractometer. The straight base line and the sharp peaks of the diffractogram confirmed that the product was well crystallized. The XRD patterns indicated that HAp was formed in this sample, and traces of other calcium phosphate impurities were not detected by this technique. The XRD pattern of sintered samples can be completely indexed with HAp in the standard card (JCPDS No. 09-0432), the only phase found present. No processing residue or secondary phases were found in the materials. TEM analysis was used to examine and estimate of HAp crystallites. TEM micrograph of

the HAp powder in is shown in Fig. 1 (b). The crystalline structure of the HAp particles has an elliptical shape with a grain size in the range of 8–12 nm.

The result of measurement of elemental composition (Ca and P content) and Ca/P molar ratio were chemically analyzed by quantitative chemical analysis via EDTA titration technique and AAS. The Ca and P content and bulk Ca/P molar ratio was determined as 38.63 (wt%), 17.48 (wt%) and 1.71, respectively. The measured Ca/P ratio for this synthesized powder was higher than stoichiometric ratio (1.667) expected for a pure HAp phase that can arise from local presence of carbonate apatite in which the Ca/P molar ratio can be as high as 3.33 [18].

3.2. Nanocomposite scaffolds

3.2.1. SEM observations

Fig. 2 shows the morphologies of the PCL, GEL and nanocomposite layers in different aspects. The

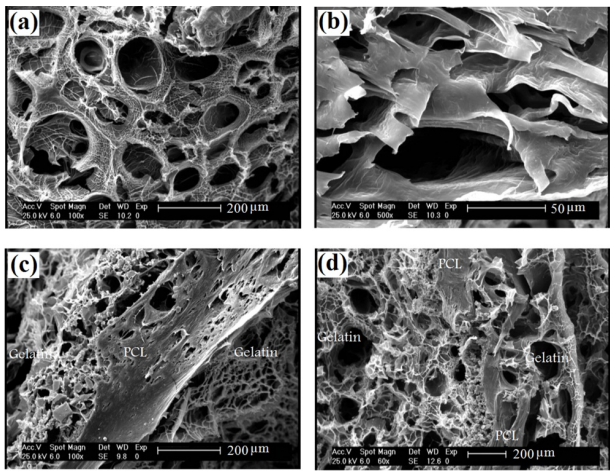

Fig. 2: The SEM micrographs of (a) the GEL layer in the nanocomposite containing 20% wt PCL, (b) the PCL layer in the nanocomposite containing 20% wt PCL, c) the GEL-PCL boundary in the nanocomposite containing 20% wt PCL, (d) the continuity of the GEL layers in the nanocomposite containing 20% wt PCL

morphological analysis of the GEL layers showed a uniform distribution of pores with an average size around 150 µm which is shown in Fig. 2 (a). Also, it can be seen that pores are either interconnected or separated via thin walls. During the fabrication process, it was expected that the HAp nanoparticles distributed homogeneously throughout the GEL network because the distribution of the HAp particles is not affected by gravity due to the keeping of the viscous GEL in an ultrasonic place and rapid freezing to form a homogeneous nanocomposite layer. According to Fig. 2 (b), a porous structure is even seen in PCL layers, especially in areas away from the GEL-PCL boundary. The pores configurations in the PCL layers are more complex and the pore size is nearly smaller which is approximately 50 µm. it is notable that, the PCL and GEL layers are mechanically bound in most areas to form GEL-PCL boundary which is shown in Fig. 2 (c) and (d). As it was mentioned previously, evaporation of acetone during the lamination technique, let macro-pores of the PCL layers make the GEL layers continuity possible throughout the nanocomposite scaffolds.

3.2.2. FTIR analyses and chemical bonds

In order to study the chemical bonds in the nanocomposite scaffolds, FTIR results obtained from two samples were investigated. Fig. 3 shows the FTIR spectra of the samples with 20 %wt PCL and 50 %wt PCL, which gives information about detected chemical bonds due to appeared peaks. The FTIR spectra of 20 %wt PCL were nearly same as that of 50 %wt PCL. There are three series of obtained peaks like 1236, 1450, 1555, 1670, 2930, 3048 cm^{-1} related to GEL, peaks at 560, 868, 1040, 3558 related to the HAp chemical structure, and also Infrared spectra for PCL-related stretching modes which were observed for both scaffold samples including 2930, 2870, 1670, 1293 and 1240 cm^{-1} [19]. But there are two peaks which are related to chemical bonds that have been formed after the mixing of GEL-HAp and then cross-linking of components which are stood at about 1345 and 2363 cm^{-1}. The first one indicates formation of the chemical bond between carboxyl group from GEL and Ca^{+2} ion from HAp that has been mentioned in former studies too [20, 21].

Herein, the chemical bonding between HAp nanoparticles and GEL in the nanocomposites has three major steps. First, a critical complex reaction between Ca^{2+} ions of HAp nanoparticles and GEL molecules [22,23]. Second, the Ca^{2+} ions of complex with GEL molecules assembled with $PO4^{3-}$ ions from HAp nanoparticles, and finally, the –COOH and $–NH_2$ groups in the GEL molecule form chemical bonds with P–O and O–H groups of HAp nanoparticles, resulting in GEL chains firmly attaching to the surface of HAp nanoparticles. It is notable that, according to Minfang *et al* [24], there are two main sources of stabilization which prevent the occurrence of the HAp particles agglomeration. The first one is electrostatic stabilization, and another one is spatial stabilization. Electrostatic stabilization in the GEL-HAp solution is mainly due to adsorption of Ca^{2+} ions on the surface of HAp nanoparticles. The adsorption would produce an electrical double layer. In other words, the ionization of carboxyl is

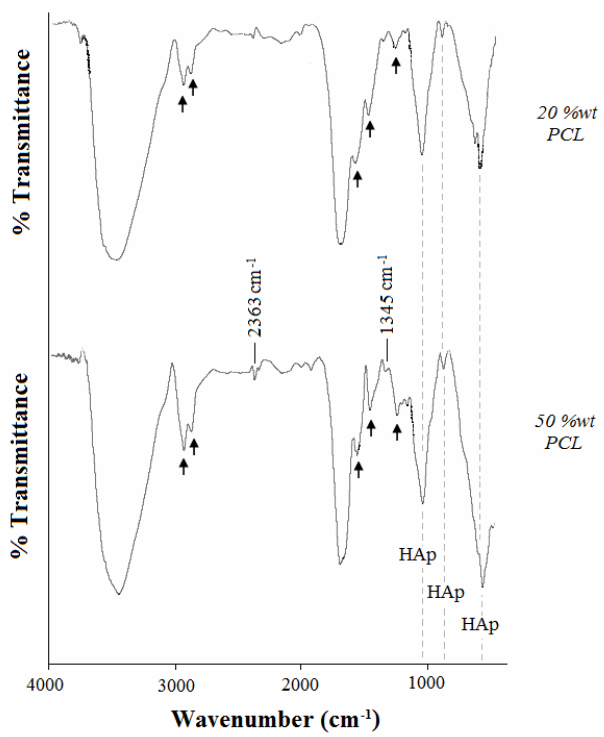

Fig. 3: The FTIR spectra of the scaffold samples in 20 %wt PCL (Top) and 50 %wt PCL (Bottom)

enforced while that of amino is restrained, and the carboxyl ions of GEL are consequently as counter ions in the electrical double layer. The spatial stabilization in this reaction system is mainly due to chemisorption of GEL molecules on the HAp nanoparticles, and GEL formed strong layers on the surface of HAp nanoparticles. Also, the bond at 2363 cm^{-1} appeared after cross-linking of GEL with GA which arises from C–H bond in C_3H_6 alkene [25]. Also, according to Ghasemi-Mobarakeh *et al* [4], PCL and GEL chains can be chemically bonded. Herein, it is worth mentioning that the appearance of the amide groups in the FTIR spectra of the nanocomposite scaffolds which is shown with arrows in Fig. 3 indicates that the PCL chains were chemically bonded

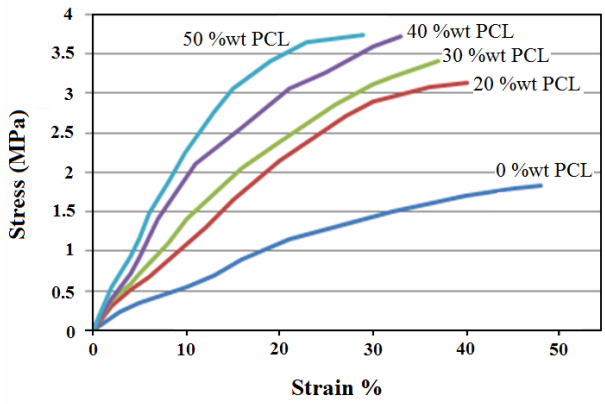

Fig. 4: The stress-strain curves of the nanocomposite scaffolds in different %wt PCL

to GEL sidewalls and it leads to the introduction of functional groups such as NH_2 and COOH on the surface of fabricated scaffolds, which was also reported by former researchers. As a conclusion, all of these chemical bonds between the elements of the fabricated scaffolds can cause a strong and effective structure for the scaffolds.

3.2.3. Mechanical properties

The mechanical properties of the fabricated porous scaffolds have been of particular concern for many tissue engineering applications due to the necessity of the structure to withstand the stress during culturing *in vitro* and as *in vivo* implants. Mechanical properties also influence specific cell functions within the engineered tissues. This is why, in the present study, compressive properties of scaffolds were examined. Fig. 4 illustrates the typical stress–strain curves for the five scaffolds prepared in this study. All the samples showed a similar stress-strain behavior (i.e., the stress increased sharply during the initial testing period, further reduced in slope).

Table 3: The mechanical properties of the nanocomposite Scaffolds.

Samples	*0% wt PCL*	*20% wt PCL*	*30% wt PCL*	*40% wt PCL*	*50% wt PCL*
$E_{0.02}$ (MPa)	8	16	19	20.5	23.5
G_{ult} (MPa)	1.83	3.13	3.40	3.71	3.73
K (N/mm)	38	79	93	114	131

As it can be seen in Table 3, the increasing of the PCL weight caused the improvement of the scaffolds mechanical properties. In addition, the elastic modulus increased from 8 MPa to 23.5 MPa for 50% wt PCL. Also, the amount of ultimate stress and Stiffness increased respectively from 1.83 MPa and 38 N/mm to 3.73 MPa and 131 N/mm. At the same time, a decrease in ultimate strain was observed according to the stress–strain curves.

3.2.4. Biomineralization evaluation

The in vitro biomineralization of the fabricated scaffolds immersed in SBF is shown in Fig. 5. The SEM micrographs showed the deposition of apatite on the surface of the scaffolds. Fig. 5 (b), (c) and (d) show the SEM micrographs of the scaffolds after immersion for 3, 7 and 14 days, respectively. According to the observations, scattered and small particles covered the surface of the scaffolds after 3 days of immersion (see Fig. 5b). After 7 days, substantial amount of apatite microparticles formed on the surfaces (see Fig. 5c). Also, after 7 days of immersion, the whole inner pore-wall surfaces of the scaffolds were covered by a layer of apatite, and the underlying surfaces were not clearly observable (Fig. 5d).

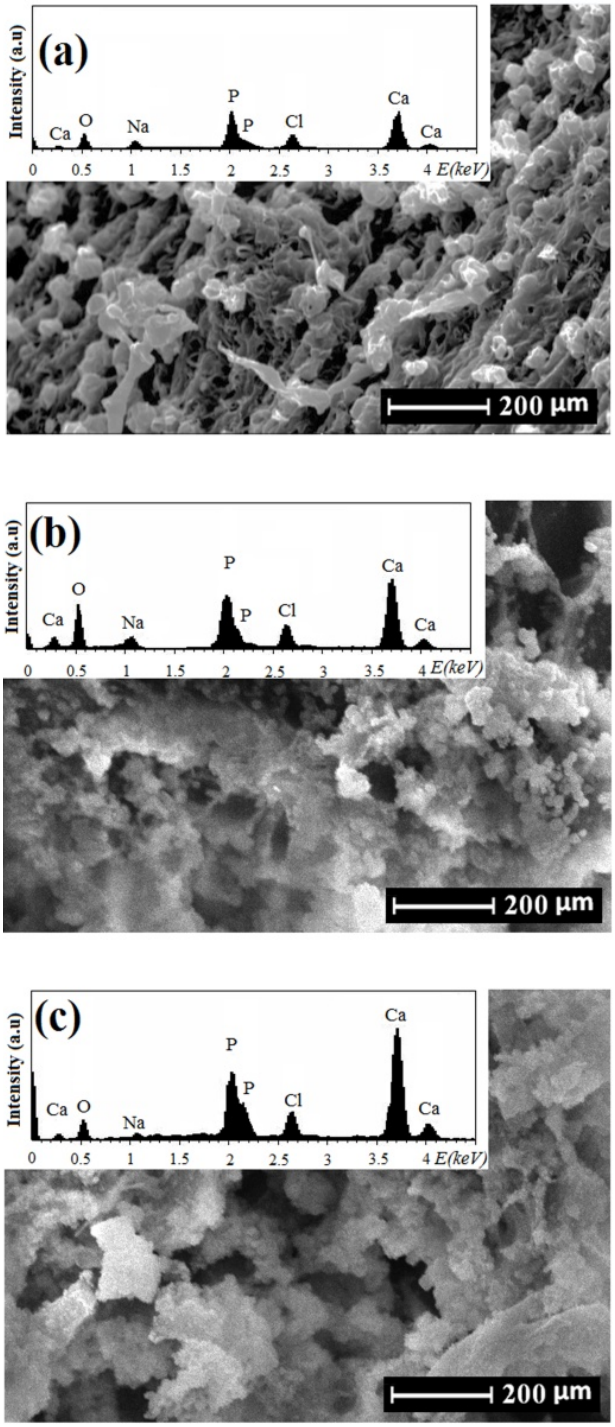

Fig. 5: The SEM-EDX micrographs of the scaffolds after immersion in SBF, (a) 3 days, (b) 7 days and (c) 14 days

We also confirmed the formation of apatite layer on the surface of scaffolds by EDX analysis, so the apparition of apatite formation on the surfaces of nanocomposite samples after immersion in SBF was established by EDX procedure, as revealed by pictures from Fig. 5. The results from EDX analysis revealed the gradual development of the apatite layer on the surfaces and pores of scaffolds after immersion in SBF solution. Furthermore, EDX analysis showed that after 14 days immersion in SBF solution, the Ca-P ratios were in accordance to nonstoichiometric biological apatite which was approximately 1.67.

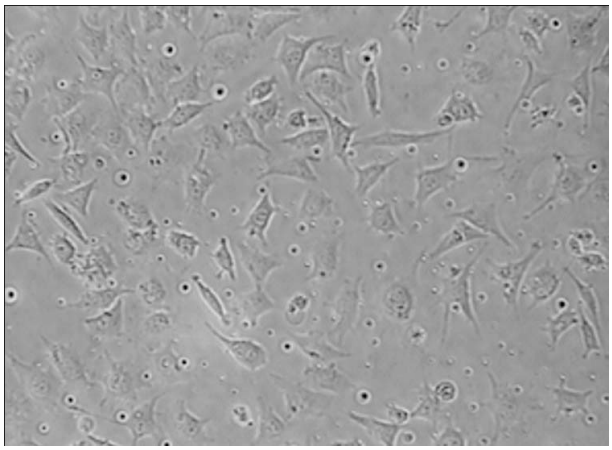

Fig. 6: The morphology of the L929 fibroblast cell lines cultured on the scaffold sample

3.2.5. Cytotoxicity evaluation

As it is seen in Fig. 6, the fabricated nanocomposite scaffolds did not show any signs of toxicity after 48 h with L929 cells. The cells appeared spindle in shape and formed a monolayer. The cytotoxic scale was measured as zero, which corresponds to non-cytotoxicity.

4. CONCLUSIONS

In this study, after testing different solvents and fabrication methods, the novel PCL-GEL-HAp nanocomposite scaffolds were successfully fabricated using a new effective lamination technique. The chemical bonds between GEL and HAp, GEL and GA, and also GEL and PCL made the scaffolds mechanically effective. The nanocomposite scaffolds were macroporous in nature and pore size ranged from 150 to 500 μm. The results from biomineralization studies revealed the gradual development of the bone-like apatite layer on the surfaces and pores of scaffolds after immersion in SBF. The Cytotoxicity evaluation results showed that the scaffolds were biocompatible. Therefore, we concluded that the PCL-GEL-HAp nanocomposite scaffold could be used as an appropriate alternative for bone tissue engineering applications.

References:

1. **Barnes, C. P., Sell, S. A., Boland, E. D., Simpson, D. G., Bowlin, G. L.**, "Nanofiber technology: Designing the next generation of tissue engineering scaffolds", *Adv. Drug Delivery Rev.,* **59** (2007), 1413-1433.
2. **Blackwood, K. A., McKean, R., Canton, I., Free-**

man, C. O., Franklin, K. L., Cole, D., Brook, I., Farthing, P., Rimmer, S., Haycock, J. W., Ryan, A. J., MacNeil, S., "Development of bio- degradable electrospun scaffolds for dermal replacement", *Biomaterials,* **29** (2008), 3091-3104.

3. **Choi, J. S., Lee, S. J., Christ, G. J., Atala, A., Yoo, J. J.,** "The influence of electrospun aligned poly(varepsilon-caprolactone)/collagen nanofiber meshes on the formation of self-aligned skeletal muscle myotubes", *Biomaterials,* **29** (2008), 2899-2906.
4. **Ghasemi-Mobarakeh, L., Prabhakaran, M. P., Morshed, M., Nasr-Esfahani, M. H., Ramakrishna, S.,** "Electrospun poly(3-caprolactone)/gelatin nanofibrous scaffolds for nerve tissue engineering", *Biomaterials,* **29** (2008), 4532-4539.
5. **Mozafari, M., Moztarzadeh, F., Rabiee, M., Azami, M., Nezafati, N., Moztarzadeh, Z., Tahriri, M.,** "Development of 3D bioactive nanocomposite scaffolds made from gelatin and nano bioactive glass for biomedical applications", *Adv. Compos Lett,* **19** (2010) 91-96.
6. **Guidoin, R., Marceau, D., Rao, T.J., King, M., Merhi, Y., Roy, P.E., Martin, L., Duval, M.,** "*In vitro* and *in vivo* characterization of an impervious polyester arterial prosthesis: The Gelseal Triaxial_ graft", *Biomaterials,* **8** (1987), 433– 441.
7. **Jonas, R.A., Ziemer, G., Schoen, F.J., Britton, L., Castaneda, A.R.,** "A new sealant for knitted Dacron prostheses minimally crosslinked gelatin", *J. Vasc Surg,* **7** (1988), 414–419.
8. **Tabata, Y., Hijikata, S., Ikada, Y.,** "Enhanced vascularization and tissue granulation by basic fibroblast growth factor impregnated in gelatin hydrogels", *J. Control Release,* **31** (1994), 189 –199.
9. **Ulubayram, K., Cakar, A.N., Korkusuz, P., Ertan, C., Hasirci, N.,** "EGF containing gelatin-based wound dressings" *Biomaterials*, **22** (2001), 1345–1356.
10. **Bezwada, R.S., Jamiolkowski, D.D., Lee, I., Vishvaroop, A., Persivale, J., Treka-Benthin, S., Erneta, M., Suryadevara, J., Yang, A., Liu, S.,** "Monocryl suture, a new ultra-pliable absorbable monofilament suture" *Biomaterials*, **16** (1995), 1141–1148.
11. **Darney, P.D., Monroe, S.E., Klaisle, C.M., Alvarado, A.,** "Clinical evaluation of the Capronor contraceptive implant—preliminary report", *Am. J. Obstet. Gynecol.,* **160** (1989), 1292–1295.
12. **Kweon, H.Y., Yoo, M.K., Park, I.K., Kim, T.H., Lee, H.C., Lee, H.S., Oh, J.S., Akaike, T., Cho, C.S.,** "A novel degradable polycaprolactone network for tissue engineering", *Biomaterials,* **24** (2003), 801– 808.
13. **Mozafari, M., Moztarzadeh, F., Tahriri, M.,** "Investigation of the physico-chemical reactivity of a mesoporous bioactive SiO2–CaO–P2O5 glass in simulated body fluid", *J Non-Cryst Solids*, **356** (2010) 1470-1478.
14. **Kikuchi, M., Itoh, S., Ichinose, S., Shinomiya, K., Tanaka, J.,** "Self-organization mechanism in a bone-like hydroxyapatite/collagen nanocomposite synthesized in vitro and its biological reaction in vivo", *Biomaterials,* **22** (2001), 1705-11.
15. **Causa, F., Netti, P.A., Ambrosio, L., Ciapetti, G., Baldini, N., Pagani, S., Martini, D., Giunti, A.,** "Poly-α-caprolactone/hydroxyapatite composites for bone regeneration: in vitro characterization and human osteoblast response", *J. Biomed Mater Res Part A.,* **76** (2006), 151-162.
16. **Chang, M.C., Ko, C.C, Douglas, W.H.,** "Preparation of hydroxyapatite-gelatin nanocomposite", *Biomaterials,* **24** (2003), 2853–2862.
17. **Liu, X., Smith, L.A., Hu, J., Maa, P.X.,** "Biomimetic nanofibrous gelatin/apatite composite scaffolds for bone tissue engineering", *Biomaterials,* **30** (2009), 2252–2258.
18. **Wei, M., Evans, J.H., Bostrom, T., Grondahl, L.,** "Synthesis and characterization of hydroxyapatite, fluoride-substituted hydroxyapa- tite and fluorapatite", *J. Mater. Sci.: Mater. Med.,* **14** (2003), 311-320.
19. **Catledge, S.A., Clem, W.C., Shrikishen, N., Chowdhury, S., Stanishevsky, A.V., Koopman, M.,** "An electrospun triphasic nanofibrous scaffold for bone tissue engineering", *Biomedical Materials,* **2** (2007), 142–50.
20. **Itoh, S., Kikuchi, M., Koyama, Y., Matumoto, H.N., Takakuda, K., Shinomiya, K.,** "Development of a novel biomaterial, hydroxyapatite/collagen (HAp/Col) composite for medical use", *J. Biomed. Mater. Eng.,* **15** (2005), 29-41.
21. **Masanori, K.B., Hiroko, N., Matsumotob, C., Takeki, Y., Yoshihisa, K., Kazuo, T., Junzo, T.,** "Glutaraldehyde cross-linked hydroxyapatite/collagen self-organized nanocomposites", *Biomaterials,* **25** (2004), 63-69.
22. **Teng, S., Shi, J., Peng, B., ChenF, L.,** "The effect of alginate addition on the structure and morphology of hydroxyapatite/gelatin Nanocomposites", *Compos. Sci. Technol.,* **66** (2006), 1532-1538.
23. **Chang, M. C., Ko, C.C., Douglas, W.H.,** "Conformational change of hydroxyapatite-gelatin nanocomposite by glutaraldehyde", *Biomaterials,* **24** (2003), 3087–3094.
24. **Minfang, C., Junjun, T., Yuying, L., Debao, L.,** "Preparation of Gelatin coated hydroxyapatite nanorods and the stability of its aqueous colloidal", *Applied Surface Science,* **254** (2008), 2730-2735.
25. **Azami, M., Moztarzadeh, F. and Tahriri, M.,** "Preparation, characterization and mechanical properties of controlled porous gelatin/hydroxyapatite nanocomposite through layer solvent casting combined with freeze-drying and lamination techniques", *J. Porous Mater., Jul* (2009) DOI 10.1007/s10934-009-9294-3.